

# Catalytic Roles of Copper on Chlorination of Precursor Phenol for Dioxins Using Ab Initio Molecular Orbital Method

Mitsuhiro Hirota\*, Takashi Araki\* and Akio Fuwa

Department of Material Science and Engineering, School of Science and Engineering, Waseda University, Tokyo 169-8555, Japan

In this study, we have clarified the chlorination mechanism of precursor phenol in the homogeneous and heterogeneous phase using ab initio molecular orbital calculation. Simultaneously, we have analyzed the catalytic roles of copper on this chlorination reaction. The results obtained in this study are as follows: (1) the chlorination of precursor phenol in the homogeneous phase progresses via the direct condensation of phenol and  $\text{Cl}_2$ , whereby desorbing  $\text{HCl}$ , (2) the chlorination of precursor phenol in the heterogeneous phase occurs via the adsorption and surface reaction of precursor phenol. The catalytic role of copper on the chlorination of precursor phenol is that  $\text{Cl-Cl}$  bond strength is weakened due to the back donation from copper surface.

(Received June 21, 2001; Accepted August 3, 2001)

**Keywords:** dioxins, catalyst, copper, ab initio molecular orbital calculation

## 1. Introduction

In recent years, the dioxins (a generic term for polychlorinated dibenzo-*p*-dioxins (PCDDs), polychlorinated dibenzo-furans (PCDFs) and polychlorinated biphenyls (PCBs)) have been given much attention as one of the most serious environmental problems owing to their acute and chronic toxicity. Urban waste incineration and pyro-metallurgical processes for metal scrap are major sources of these dioxins formation and emission. Thus, the countermeasure to these processes becomes urgency. These dioxins can be decomposable under the high temperature and high oxygen potential,<sup>1,2)</sup> although polychlorinated phenols and benzenes have not been decomposed in this condition. These dioxin precursor substances have been believed to lead the dioxins formation by the catalytic roles of heavy metal such as copper and its compounds on fly ashes.<sup>3)</sup> Moreover, the heavy metals have the catalytic roles on the formation of chlorination sources and the chlorination of precursor substances as well. There have been many experimental studies for the dioxins formation in the heterogeneous phase,<sup>4-10)</sup> but the dioxins formation mechanism has not yet been clarified to any great extent. Since the experimental analysis of the dioxins requires precision in measurement on the order of less than parts per billion, theoretical studies for the dioxins formation have been active in recent years. Ritter and *et al.* analyzed the pathway to PCDD/F from partial oxidation of chlorinated aromatic by thermodynamics and kinetics.<sup>11)</sup> Okamoto and *et al.* discussed the formation pathways from 2,4,5-trichlorophenol to PCDDs in the homogeneous phase using ab initio molecular orbital calculation.<sup>12)</sup> The heterogeneous reaction analysis has been needed in order to understand the dioxins formation in the urban waste incineration and pyro-metallurgical processes for metal scrap. In our previous work, we analyzed the catalytic role of copper on the dibenzo-*p*-dioxin (DD) formation using ab initio molecular orbital calculation.<sup>13)</sup>

In such situation, we have focused and studied the chlorination of the dioxins precursor substances in the heterogeneous

phase, because the toxicity of the dioxins is strongly dependent on substitution chlorine atom of them. Thus, it is our aim of this study to clarify the chlorination mechanism of precursor phenol in the homogeneous and the heterogeneous phase and to analyze the catalytic roles of copper on this chlorination using ab initio molecular orbital calculation.

## 2. Computational Details

### 2.1 Ab initio molecular orbital calculation

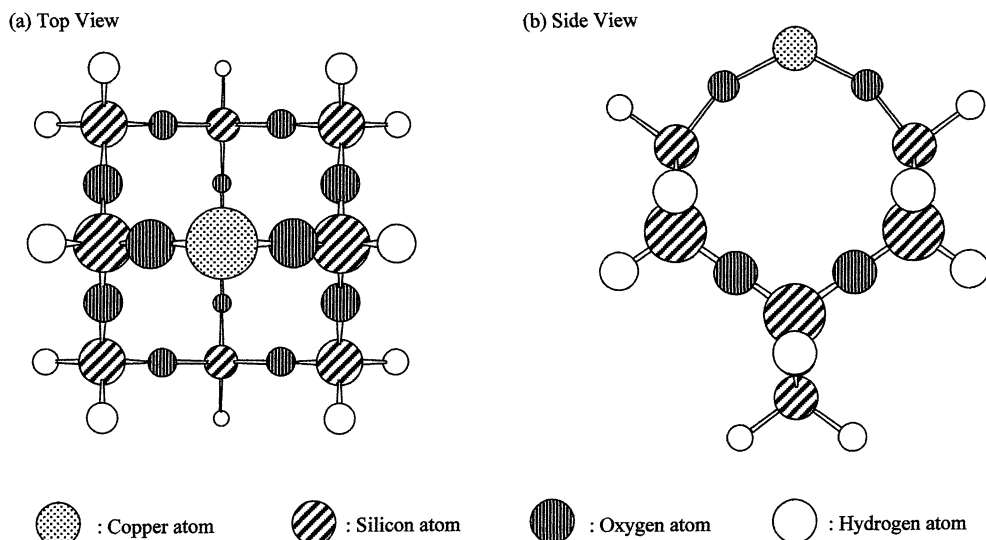
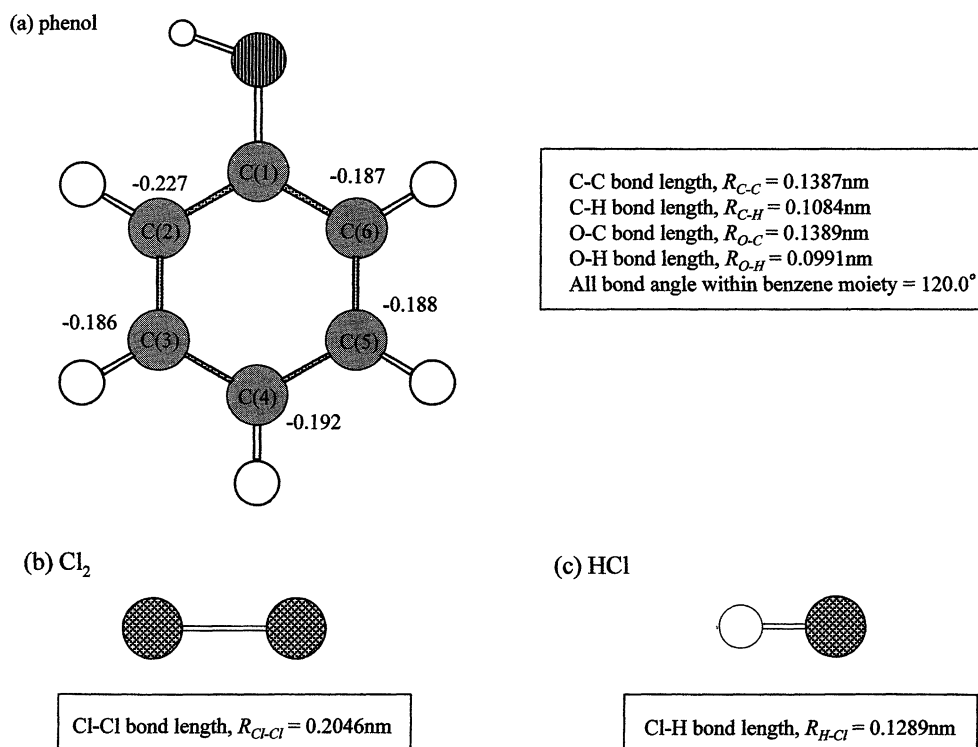
Ab initio molecular orbital calculations were performed using the Gaussian98 program package.<sup>14)</sup> The total energy and the optimized geometry were determined by the hybrid density functional method (UB3LYP).<sup>15-18)</sup> For hydrogen, carbon, oxygen, chlorine or silicon atom, the standard 3-21g\* basis set was used. For copper atom, the Neon core was replaced by the Hay and Wadt's effective core potential,<sup>19)</sup> while valence 3s3p3d4s electrons were treated explicitly by the Gaussian basis function of double zeta quality. Then, the transition state was confirmed by harmonic vibration analysis and intrinsic reaction coordinate calculation.

### 2.2 Cluster model

In the urban waste incinerator, the copper has adsorbed on the fly ashes in which  $\text{SiO}_2$  is one of the main components.<sup>20)</sup> Thus, we assumed copper on the fly ashes by Cu- $\text{SiO}_2$  cluster model. Figure 1 shows the geometry of this cluster model. The geometry of this cluster is decided according to the following procedures:

- (1) The geometrical parameters for  $\text{SiO}_2$ , which has the  $\beta$ -cristobalite structure, are fixed at its experimental values.<sup>21)</sup>
- (2) The dangling bond of silicon atom is terminated by hydrogen atom so that the valence electron of silicon atom forms  $sp^3$  hybrid orbital.
- (3) The copper is placed on the hollow bridge site. Then, the geometrical parameters for copper and oxygen atom at hollow bridge site are optimized using ab initio molecular orbital calculation.

\*Graduate Student, Waseda University.

Fig. 1 The geometry of Cu-SiO<sub>2</sub> cluster with C<sub>2v</sub> symmetry.Fig. 2 The optimized geometry of phenol, Cl<sub>2</sub> and HCl at ground state.

This Cu-SiO<sub>2</sub> cluster model can perform the lower calculation cost compared with the cluster consist of only copper atom. Namely, the analysis of the chlorination of precursor phenol in the heterogeneous phase using the larger size cluster becomes possible. Thus, the electronic state of this cluster can be accurately described. Moreover, the structural relaxation by adsorption and surface reaction can be also considered. These advantages are necessary in order to achieve our aim of this study.

### 3. Result and Discussion

#### 3.1 Chlorination of precursor phenol in the homogeneous phase

In this section, we analyze the chlorination of precursor phenol in the homogeneous phase. In urban waste incinerator and pyro-metallurgical processes, HCl, which is included at the high concentration in the exhaust gas, forms chlorination source Cl<sub>2</sub> via *Deacon reaction*.<sup>3)</sup> Thus, the chlorination of precursor phenol in the homogeneous phase is as follows:

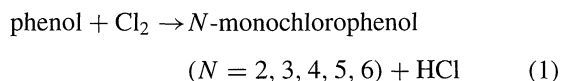


Figure 2 shows the optimized geometry of phenol,  $\text{Cl}_2$  and  $\text{HCl}$  at ground state, respectively. All geometrical parameters of these molecules are in good agreement with experimental values.<sup>22,23</sup> Figures 3, 4 and 5 show the electronic configurations and schematic illustration of respective MOs of phenol,  $\text{Cl}_2$  and  $\text{HCl}$ , respectively. The eigenvalue of  $\sigma[\text{Cl}-\text{Cl}]$  orbital is less stable than that of  $\sigma[\text{H}-\text{Cl}]$  orbital. Namely, the reactivity of  $\text{Cl}_2$  is higher than that of  $\text{HCl}$ .

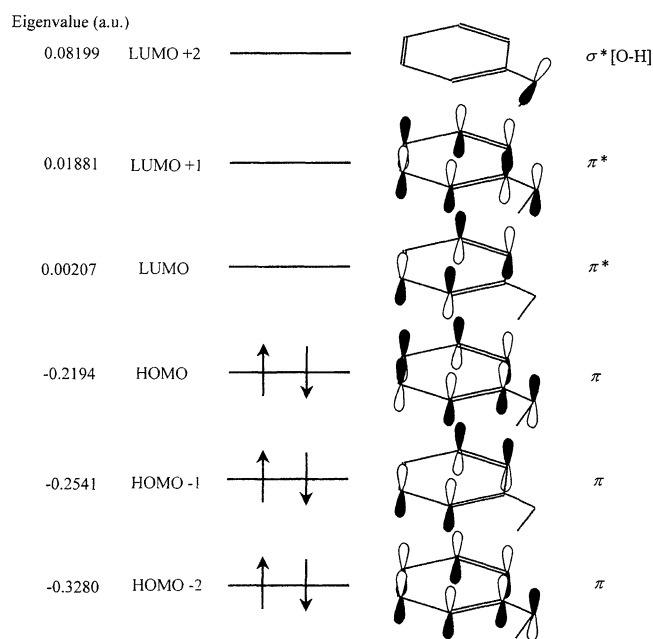


Fig. 3 The electronic configuration and schematic illustration of respective MOs of phenol.

Figures 6 and 7 show the optimized geometry at transition state in  $N$ -monochlorophenol ( $N = 3, 4, 5, 6$ ) formation and the optimized geometry of 4-monochlorophenol at ground state, respectively. No transition state in the chlorination reaction to produce 2-monochlorophenol exists because of high steric effect of hydroxy group. In Figure 6(b),  $R_{\text{Cl}-\text{Cl}}$  increases from 0.2046 ( $\text{Cl}_2$ ) to 0.2691 nm (TS).

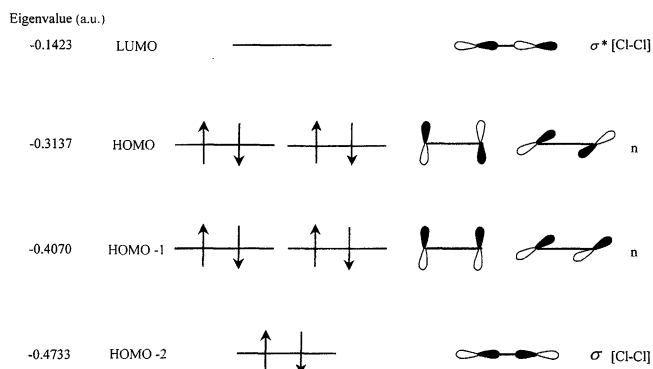


Fig. 4 The electronic configuration and schematic illustration of respective MOs of  $\text{Cl}_2$ .

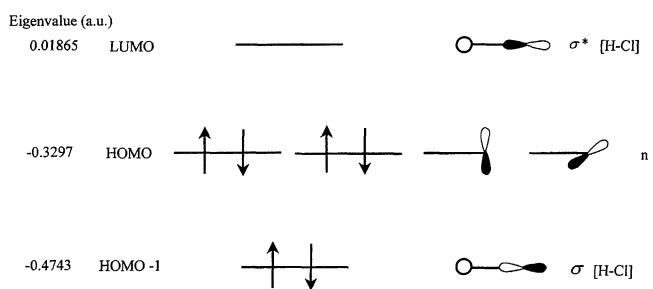


Fig. 5 The electronic configuration and schematic illustration of respective MOs of  $\text{HCl}$ .

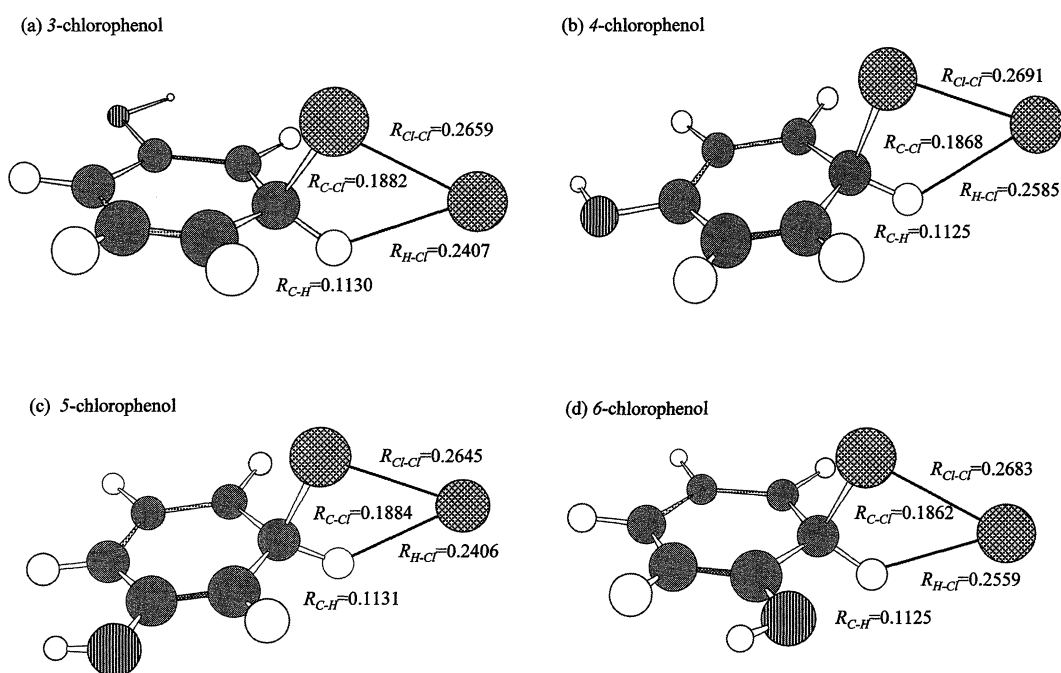
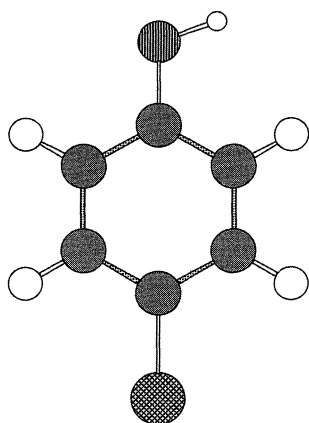


Fig. 6 The optimized geometry at transition state in  $N$ -monochlorophenol ( $N = 3, 4, 5, 6$ ) formation.



C-C bond length,  $R_{C-C} = 0.1395\text{nm}$   
 C-H bond length,  $R_{C-H} = 0.1083\text{nm}$   
 O-C bond length,  $R_{O-C} = 0.1389\text{nm}$   
 O-H bond length,  $R_{O-H} = 0.0991\text{nm}$   
 C-Cl bond length,  $R_{C-Cl} = 0.1762\text{nm}$   
 All bond angle within benzene moiety =  $120.0^\circ$

Fig. 7 The optimized geometry of 4-monochlorophenol at ground state.

Table 1 The activation energy of the chlorination for *N*-monochlorophenol ( $N = 2, 3, 4, 5, 6$ ).

Products	Activation energy, $E_a/\text{kJ}\cdot\text{mol}^{-1}$
2-monochlorophenol	no transition state
3-monochlorophenol	296.1
4-monochlorophenol	196.6
5-monochlorophenol	301.6
6-monochlorophenol	262.5

and  $R_{C-H}$  from 0.1084 (phenol) to 0.1125 nm (TS), respectively. In contrast,  $R_{C-Cl}$  decreases from 0.1868 (TS) to 0.1762 nm (4-monochlorophenol) and  $R_{H-Cl}$  from 0.2585 (TS) to 0.1289 nm (HCl). The similar tendency in geometrical parameters can be seen in Figs. 6(a), (c) and (d). These results clearly show that the both Cl-Cl and C-H bonds break, and the both C-Cl and H-Cl bonds form during the chlorination. Namely, the chlorination of precursor phenol in the homogeneous phase progresses via the direct condensation of phenol and  $\text{Cl}_2$ , whereby desorbing HCl. Table 1 shows the activation energy of reaction (1) for these five isomers. The activation energy of the chlorination to produce 4-monochlorophenol is the lowest. This is because C(4) atom has the largest negative charge of all carbon atom except for C(2) atom (shown in Fig. 2(a)). Namely, the charge transfer between C(4) and Cl atom, which promotes the Cl-Cl bond breaking, superiorly occurs. From the above-mentioned results, we conclude that the structural factor, which decides the reactivity of the chlorination of precursor phenol, is Cl-Cl bond.

### 3.2 Chlorination of precursor phenol in the heterogeneous phase

In this section, we analyze the catalytic roles of copper on the chlorination of precursor phenol. The

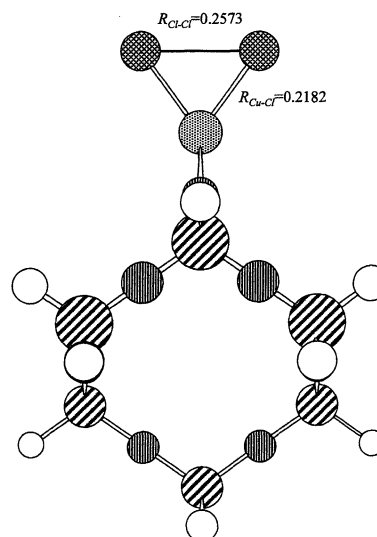


Fig. 8 The optimized geometry of  $\text{Cl}_2$  on the cluster.

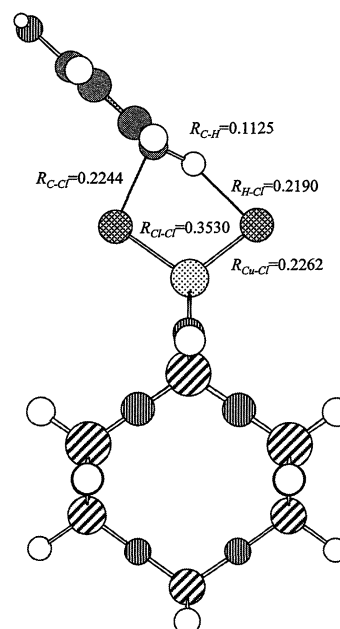


Fig. 9 The optimized geometry of phenol on the cluster.

4-monochlorophenol, which is formed via minimum energy path in the homogeneous phase, is chosen as a product of this chlorination. Thus, the chlorination of phenol in the presence of copper is here proposed to occur the following sequences:

- (1) Adsorption of  $\text{Cl}_2$  onto the cluster.
- (2) Adsorption of phenol onto the cluster.
- (3) 4-monochlorophenol formation desorbing HCl on the cluster.

Figure 8 shows the optimized geometry of  $\text{Cl}_2$  on the cluster. In Fig. 8,  $R_{Cl-Cl}$  increases from 0.2046 to 0.2573 nm in this adsorption. This result indicates that  $\text{Cl}_2$  performs dissociative adsorption on the cluster. This dissociation progresses through the back donation from the cluster to  $\sigma^*[\text{Cl-Cl}]$  orbital of  $\text{Cl}_2$ . The dissociated Cl atom has the large negative charge and the high reactivity. Figures 9 and 10 show the optimized geometry of phenol on the cluster and the optimized

geometry at transition state in 4-monochlorophenol formation on the cluster, respectively. In Fig. 9,  $R_{C-H}$  increases from 0.1084 (phenol) to 0.1125 nm (adsorbed phenol). This is because the  $\pi$  electron delocalized in benzene moiety of phenol becomes localized in carbon atom at *para* site thorough charge transfer from Cl atom. In brief, the  $sp^2$  hybrid orbital, which formed the benzene ring, collapses by this adsorption, thereby C-H bond being weakened. In Fig. 10, both  $R_{H-Cl}$  decreases from 0.2190 (adsorbed phenol) to 0.2108 nm (TS) and  $R_{C-Cl}$  from 0.2244 (adsorbed phenol) to 0.1867 nm (TS). This is because adsorbed Cl atom can move like a Cl radical, which has the high reactivity, by the above-mentioned back donation from the cluster. Namely, HCl desorbing from the

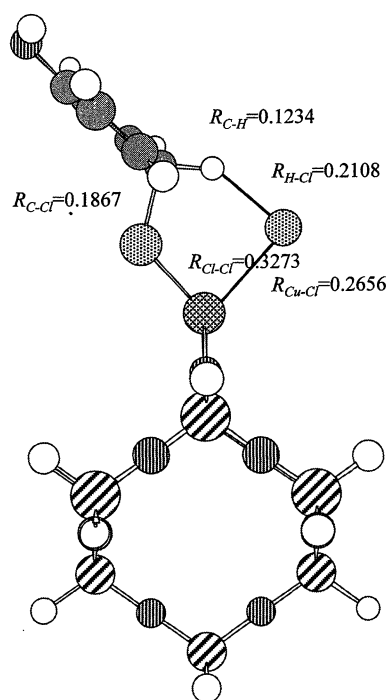


Fig. 10 The optimized geometry at transition state of the chlorination of precursor phenol on the cluster.

cluster easily take place compared to that in the homogeneous phase. With this desorbing, the benzene moiety rebuilds  $sp^2$  hybrid orbital and 4-monochlorophenol is formed on the cluster. Figure 11 shows the total energy profiles of the chlorination of precursor phenol in the respective homogeneous and heterogeneous phase. The apparent activation energy of the chlorination of phenol in the heterogeneous phase is lower than that in the homogeneous phase. Namely, the chlorination of precursor phenol is promoted by the catalytic role of copper. This catalytic role of copper on the chlorination of precursor phenol is that Cl-Cl bond strength, which decides the reactivity of this chlorination, is weakened due to the back donation from the cluster.

#### 4. Conclusion

In this work, we have clarified the chlorination mechanism of precursor phenol in the homogeneous and heterogeneous phase using ab initio molecular orbital calculation. Simultaneously, we have analyzed the catalytic roles of copper on this chlorination. In the homogeneous phase, the chlorination of precursor phenol progresses via the direct condensation of phenol and  $Cl_2$ , whereby desorbing HCl. The structural factor, which decides the reactivity of this chlorination, is Cl-Cl bond. In the presence of copper, the chlorination of precursor phenol occurs the following sequences: (1) adsorption of  $Cl_2$  onto the cluster, (2) adsorption of phenol onto the cluster, and (3) monochlorophenol formation desorbing HCl on the cluster. The catalytic role of copper on the chlorination of precursor phenol is that Cl-Cl bond strength, which decides the reactivity of this chlorination, is weakened due to the back donation from the cluster.

#### Acknowledgements

This research was partially supported by the Ministry of Education, Science, Sports and Culture, Grant-in-Aid for Scientific Research (B), 11555195, 1999.

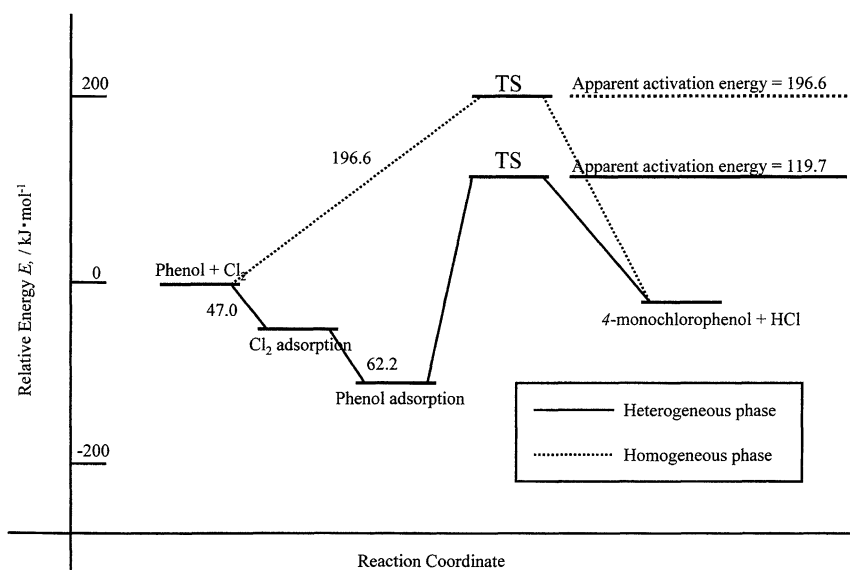


Fig. 11 The total energy profiles of the chlorination of precursor phenol in the homogeneous and heterogeneous phases.

## REFERENCES

- 1) N. Saito, T. Ishizaki and A. Fuwa: *Toxic. Environ. Chem.* **74** (1999) 165–177.
- 2) N. Saito, T. Ishizaki and A. Fuwa: *Toxic. Environ. Chem.* **75** (2000) 161–179.
- 3) R. Addink, B. V. Bavel, R. Visser, H. Wever, P. Slot and K. Olie: *Chemosphere* **20** (1990) 1929–1934.
- 4) K. Ballschmiter and M. Swevev: *Fresenius Anal. Chem.* **328** (1987) 125–127.
- 5) K. Ballschmiter, I. Braunmiller, R. Niemczyk and M. Swevev: *Chemosphere* **17** (1988) 995–1005.
- 6) J. Cole, J. D. Bittner, J. Longwell and J. Howard: *Combust and Flame* **56** (1984) 51–70.
- 7) R. D. Griffin: *Chemosphere* **15** (1986) 1987–1989.
- 8) F. W. Karasek and L. C. Dickson: *Science* **237** (1987) 754–756.
- 9) F. W. Karasek and L. C. Dickson: *J. Chromatography* **389** (1987) 127–137.
- 10) T. Lippert, A. Wolkum and D. Lenmair: *Environ. Sci. and Technol.* **25** (1991) 1485–1489.
- 11) E. R. Ritter and J. W. Bozzelli: *Combust. Sci. and Tech.* **101** (1994) 153–169.
- 12) Y. Okamoto and M. Tomonari: *J. Phys. Chem.* **103** (1999) 7686–7691.
- 13) N. Saito, M. Hirota, T. Ishizaki and A. Fuwa: *Second International Conference on Processing Materials for Properties*, (San Francisco, California, 2000) pp. 727–732.
- 14) Gaussian 98 (Revision A.7), M. J. Frisch, G. W. Trucks, H. B. Schlegel, G. E. Scuseria, M. A. Robb, J. R. Cheeseman, V. G. Zakrzewski, J. A. Montgomery, R. E. Stratmann, J. C. Burant, S. Dapprich, J. M. Millam, A. D. Daniels, K. N. Kudin, M. C. Strain, O. Farkas, J. Tomasi, V. Barone, M. Cossi, R. Cammi, B. Mennucci, C. Pomelli, C. Adamo, S. Clifford, J. Ochterski, G. A. Petersson, P. Y. Ayala, Q. Cui, K. Morokuma, D. K. Malick, A. D. Rabuck, K. Raghavachari, J. B. Foresman, J. Cioslowski, J. V. Ortiz, B. B. Stefanov, G. Liu, A. Liashenko, P. Piskorz, I. Komaromi, R. Gomperts, R. L. Martin, D. J. Fox, T. Keith, M. A. Al-Laham, C. Y. Peng, A. Nanayakkara, C. Gonzalez, M. Challacombe, P. M. W. Gill, B. G. Johnson, W. Chen, M. W. Wong, J. L. Andres, M. Head-Gordon, E. S. Replogle and J. A. Pople: Gaussian, Inc. Pittsburgh PA (1998).
- 15) A. D. Becke: *J. Chem. Phys.* **98** (1993) 1372–1377.
- 16) A. D. Becke: *J. Chem. Phys.* **98** (1993) 5648–5652.
- 17) C. Lee, W. Yang and R. G. Parr: *Phys. Rev.* **B37** (1988) 785–789.
- 18) R. G. Parr and W. Yang: *Density functional theory of atoms and molecules*, (Oxford University Press, Oxford, 1989) pp. 47–66.
- 19) P. J. Hay and W. R. Wadt: *J. Chem. Phys.* **82** (1985) 270–283.
- 20) K. J. Carolyn and H. A. Ronald: *Environ. Sci. Technol.* **26** (1992) 502–507.
- 21) D. M. Hatch and S. Ghose: *Phys. Chem. Minerals* **17** (1991) 554–562.
- 22) N. W. Larsen: *J. Mol. Struct.* **51** (1979) 175–190.
- 23) K. P. Huber and G. Herzberg: *Molecular Spectra and Molecular Structure, Vol. 4, Constants of Diatomic Molecules*, (Van Nostrand Reinhold, New York, 1979) pp. 146–291.